Diffusion of induced currents during EM transmitter on-time

Adam Smiarowski, Tianyou Chen[*], CGG

Summary

The electromagnetic smoke ring concept is a useful device for understanding how the fields induced in a 1-D earth propagate and diffuse in a medium. Aside from facilitating a physical understanding of field propagation, the smoke ring concept has been used to interpret behavior of vertical and radial magnetic fields at the surface (Pridmore, 1978) and used to estimate depth of penetration for conductivity-depth transforms (Sengpiel, 1988). Previous authors analyzing time-domain systems have focused their analysis on the current induced by a transmitter step-off excitation, neglecting practical airborne EM waveforms. In this paper, we study the current system induced during the on-time of a half-sine transmitter waveform and compare with the off-time current pattern. Since current is continually generated at surface, the on-time current pattern is more densely distributed near-surface than the off-time current system, suggesting that on-time field measurements should be relatively more sensitive to shallow targets.

Introduction

The concept of an expanding smoke ring has been used to illustrate the diffusion of an electric field in a layered earth. Nabighian (1979) explained how a transmitter step-off excitation induces a current system in a homogenous halfspace which diffuses outward and downward from the transmitter. Hoversten and Morrison (1982) calculated electric field contours from a repetitive square-wave system for various layered earth models, showing that the smoke-ring becomes distorted at layer boundaries. Reid and Macnae (1996) examined smoke rings for the frequency-domain case and showed the in-phase and quadrature electric fields. Yin and Hodges (2007) computed 4-D frequency-domain electric and magnetic fields, showing diffusion in anisotropic mediums. Yin and Hodges showed that the continuous sine-waveform of frequency domain systems causes alternating positive and negative wave fronts to propagate as the transmitter polarity changes. In the time-domain case, only the ideal step-off waveform has been discussed in the literature. In this work, we calculate and analyze the diffusion pattern for a half-sine waveform. In particular, we focus on the current distribution during the transmitter on-time.

Method

The electric field in a layered earth due to a vertical dipole transmitter has been discussed by a number of authors, including Morrison et al. (1969), Lee and Lewis (1973) and Singh and Mogi (2005). Following the presentation in Kaufmann and Keller (1983), the frequency-domain electric field E at a position horizontally offset from the transmitter by r and z meters deep in a layered earth can be calculated as

$$E_{\phi 1} = \frac{i\omega\mu}{8\pi} \int_0^\infty \frac{2\lambda}{\lambda+m} e^{-\lambda h} e^{-mz} J_0(\lambda r) d\lambda \qquad (1)$$

where $E_{\phi 1}$ is the azimuthally circulating electric field in the topmost layer, ω is the angular frequency in radians, h is transmitter elevation, z is depth in the layer, r is horizontal distance from the transmitter, μ is magnetic permeability of the layer, J_o is the Bessel function of order 0, and λ is the Hankel transform integration variable. We transform the electric field into the time-domain using the Fourier transform as described by Christensen (1990) and obtain the step response of the halfspace.

To obtain the electric field from a half-sine waveform, we convolve the electric field with the time-derivative of the transmitter current I(t) as

$$E(t) = I(t) * E_{IP} = -\frac{dI(t)}{dt} * E_S \qquad (2)$$

where E_{IP} is the impulse response and E_s is the step-response of the halfspace. The current density J_ϕ in the earth is calculated using Ohm's Law, $J_\phi = \sigma E_{s\phi}$, where σ is the conductivity of the earth.

To our knowledge, the only systems which acquire and interpret on-time data are AEROTEM and CGG's HELITEM[®], GEOTEM[®] and MEGATEM[®] systems. Here, we use the helicopter HELITEM system for calculations.

We place the transmitter 30 m above the surface of the earth and use a half-sine waveform with 4 ms pulse width and moment of 2 million Am^2. The waveform is shown in Figure 1; the primary field at the receiver, which measures the time rate of change of the magnetic field, is a half-cosine and shown in the bottom panel.

We calculate the current density induced in a 1 Ωm homogenous halfspace at 1 μs intervals from the start of excitation and image contours of the current density in the earth. Figures 2, 3 and 4 present current density normalized by the maximum current density at specific delay times. We show contours for 10%, 25%, 75% and 99% of the maximum current density (the 10% contour is annotated to indicate amplitude of the current density). Figure 2 shows the up-ramp phase of the half-sine waveform (time interval between 0 and 2 ms), Figure 3 shows the down-ramp interval (from 2 to 4 ms) and Figure 4 shows current density during the off-time.

The off-time current density is most similar to the step-off studies in the literature. As shown in Figure 4, current density resembles a smoke-ring with the current maximum diffusing downward and outward.

Figure 2 shows that at a short time after the turn-on of the pulse, the current is concentrated near-surface and the induced current density has opposite sign to the EM induction. Initially, current diffuses deeper into the earth as shown by the 10% contour moving deeper. Notice that 0.5 ms after turn-on, the 10% contour attains its maximum value; at 1, 1.5 and 1.75 ms, the amplitude is smaller. This is because the induction is maximum at time 0; throughout the rest of the ramp-up, induction becomes smaller. Also, notice that the 99% contour is very near-surface throughout the up ramp. For a step-off waveform, current density is initially near-surface but quickly diffuses outward and downward. In the on-time, ground is continuously energized and current is continuously generated at surface.
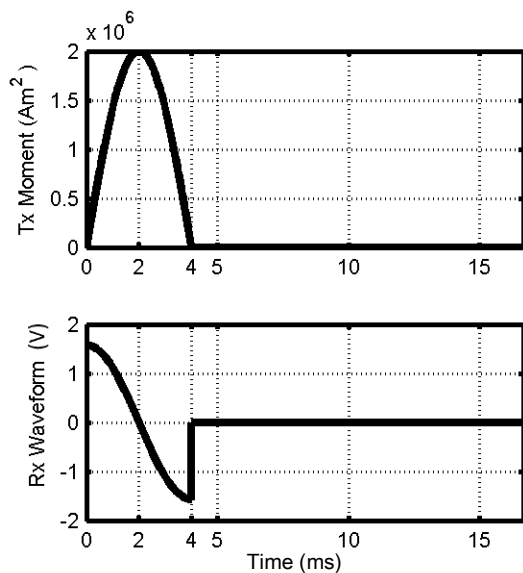

Figure 1: Transmitter current waveform (top) and corresponding dB/dt receiver waveform (created by the current waveform (bottom).

The current distribution 0.01 ms after the start of the pulse (Figure 2) is much more concentrated near-surface than current 0.01 ms after the end of the pulse in the off-time (which is the 4.01 ms panel in Figure 4). In fact, the 10% contour reaches 50 m depth 0.01 ms after the end of the pulse in the off-time but 1 ms after the start of the pulse in the on-time. This suggests that on-time data should be more sensitive to the near-surface.

Figure 3 shows current density from the mid-point of the waveform to the end of the waveform (the down-ramp). At the midpoint of the waveform, the primary excitation is 0 (as shown in receiver waveform panel in Figure 1). When the induction is zero, the location of maximum current density begins to diffuse downward and outward as shown by the 2.01 ms panel in Figure 3. The induction is now becoming negative, generating current flow in the opposite direction to that of the up-ramp of the waveform. The 2.25 ms panel shows negative current (dashed lines) at depth, with positive current flowing at surface. As time progresses, the negative current diffuses away and is replaced by positive current.

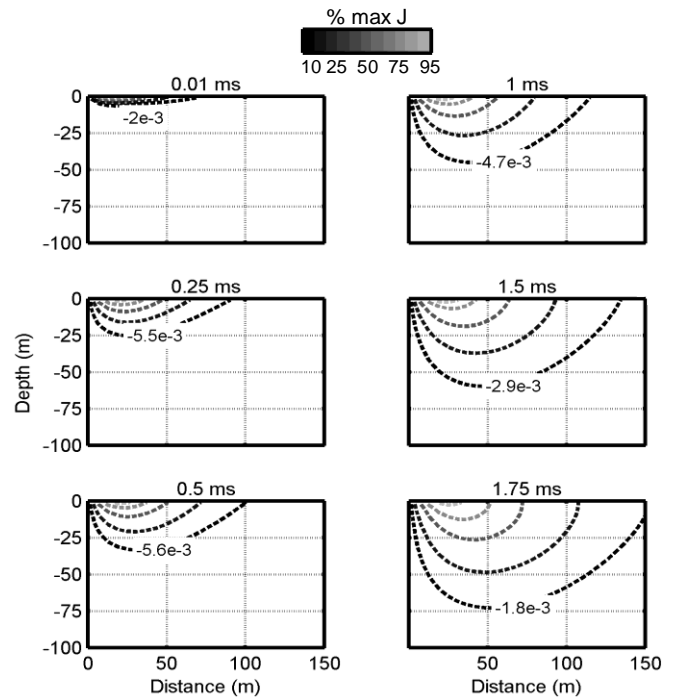During the up-ramp, there is maximum induction just after

Figure 2: Current density (A/m^2) during the up-ramp of the half-sine waveform in a 1 Ωm halfspace. Each panel has a different scale normalized to the maximum current density at that time; dashed lines indicate negative current. Contours indicate 10, 25, 75 and 99% of maximum current value. The time from beginning of turn-on is indicated above each panel.

turn-on; a large amplitude smoke-ring is generated just under the transmitter. Throughout the remainder of the up-ramp, smaller-amplitude smoke rings are created at surface. Contrast this to the down-ramp of the waveform, where induction increases from a minimum at the midpoint to a maximum at the end of the down-ramp; that is, a small-amplitude smoke ring is initially created, diffusing to depth,

while new smoke rings with large-amplitude are created at surface. Notice the almost-stationary 10% contour late on-time panels in the down-ramp shown in Figure 3. The down-ramp shows relatively greater concentration of current at shallow depths.
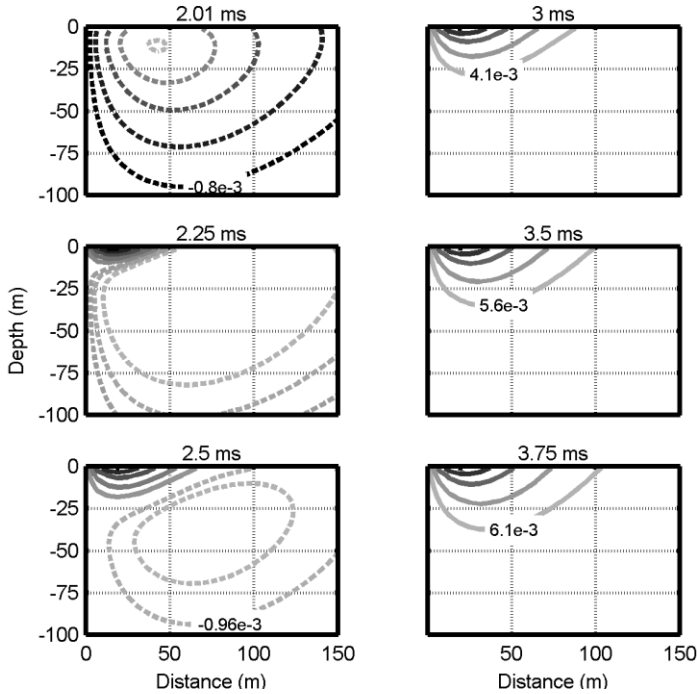

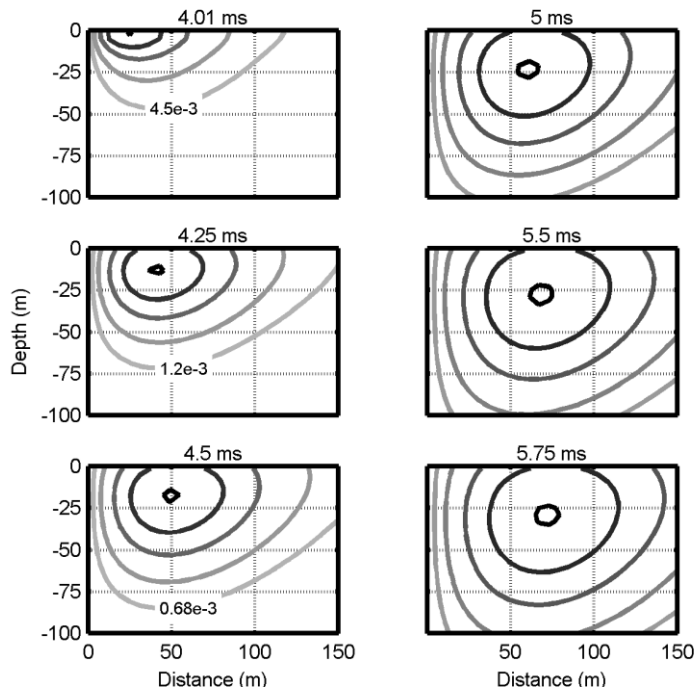Figure 3: Current density during the down-ramp interval of the half-sine waveform.

Figure 4: Current density in a 1 Ωm halfspace after a 4ms half-sine waveform excitation.

The example has shown current distribution in a 1 Ωm earth, a quite conductive example. In a resistive earth, the current diffuses away much more quickly.

Sensitivity Distribution

Here we are interested in determining how sensitivity to depth changes as a function of time for on-time measurements. We first compute the magnetic field at the receiver due to each current filament in the earth (here, the receiver is 27 m above the transmitter) using the Biot-Savart law; we call the contribution from each current filament $S(z,x,t)$, where z is depth in the ground, x is horizontal offset and t is time after the start of the pulse. The relative sensitivity of different depths can be computed by summing the contribution of all current filaments in at a particular depth at a given time.

To determine to what maximum depth a particular time channel is sensitive to, we compute a cumulative sensitivity as

$$C(z_k, t) = \frac{\sum_{i=1}^{k} \sum_{m=1}^{M} S(z_i, x_m, t)\, dx\, dz}{\sum_{i=1}^{N} \sum_{m=1}^{M} S(z_i, x_m, t)\, dx\, dz} x100 \qquad (3)$$

where C is the cumulative sensitivity for a particular depth and time, M is the number of horizontal positions and N the number of depth locations. Starting from the surface, this expression sums the contribution from all horizontal positions at that depth, and continues downward. Cumulative sensitivity is shown for a 100 Ωm earth in Figure 5 and a 1 Ωm earth in Figure 6; the contour value shows what portion of the receiver signal is due to the currents at and above that depth; we take the 90% contour as being the maximum depth of exploration.
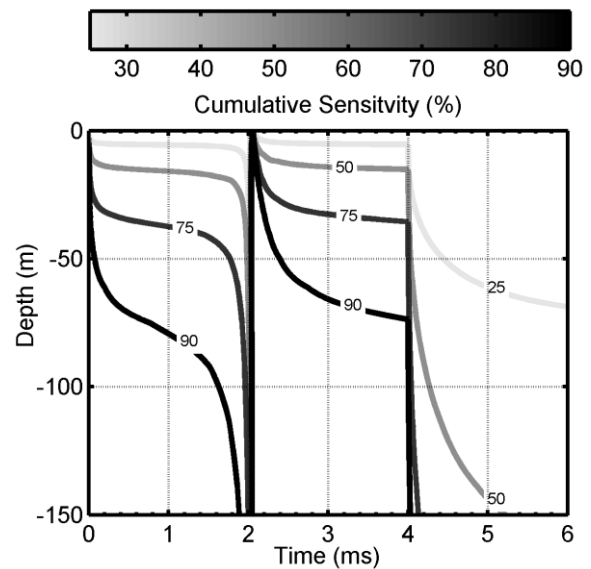

Figure 5: Cumulative sensitivity for a 100 Ωm halfspace. The contour level indicates the portion of the receiver signal due to the (magnetic fields generated by) current located from surface to that depth.

Figure 1 shows three distinct phases of the induction; induction is positive from 0-2 ms, negative from 2-4 ms and 0 afterward. The cumulative sensitivity also shows three phases where the maximum depth of exploration is increasing. Exploration depth increases after the switch-off, after the switch-on, and a transition time after the induction changes polarity. Figure 5 shows that for a relatively resistive halfspace, the transition occurs very close to when the induction changes sign.

In a conductive earth (Figure 6) current diffusion is slower and the transition time is delayed. As shown in Figure 3, current from the up-ramp is still present while the down-ramp induces current in the opposite direction.

The on-time current density is distributed much more closely to surface than at an equivalent time after the end of the pulse. For example, 10 μs after the end of the pulse in a 100 Ωm earth, 90% of the receiver signal is from current in the top 125 m. During the on-time, the 90% contour is generally shallower than 60 m. The effect is less noticeable in a conductive earth (because diffusion is slower); but current density in the early on-time is concentrated relatively more at-surface than in the early off-time.

The up-ramp and down-ramp show different depth sensitivities. We believe this is due to 2 reasons:
(1) current from the up-ramp may not have diffused away by the time of the down-ramp
(2) induction in the up-ramp starts at a maximum and decreases to zero, while during the down-ramp, induction starts from zero and goes to a maximum. The result is that during the up-ramp, a smoke ring with large amplitude fields is initially generated (which diffuses to depth); relatively small-amplitude smoke rings are subsequently generated at surface during the remainder of the up-ramp. In the down-ramp case, a small smoke ring is initially generated, with larger smoke rings being generated at surface. The result is higher current density at surface compared to depth for the down-ramp case.

Conclusions

We have calculated current density in the earth during the on-time of a half-sine waveform. The classic smoke-ring diffusion of current is distorted by the extended time over which the half-sine waveform energizes the ground. Instead of a clear propagation of the current density maximum outward and downward, near-surface current is continuously generated, replacing current that diffuses away. During the on-time current is relatively more concentrated near-surface than during the off-time. Therefore we suggest that on-time measurements should be
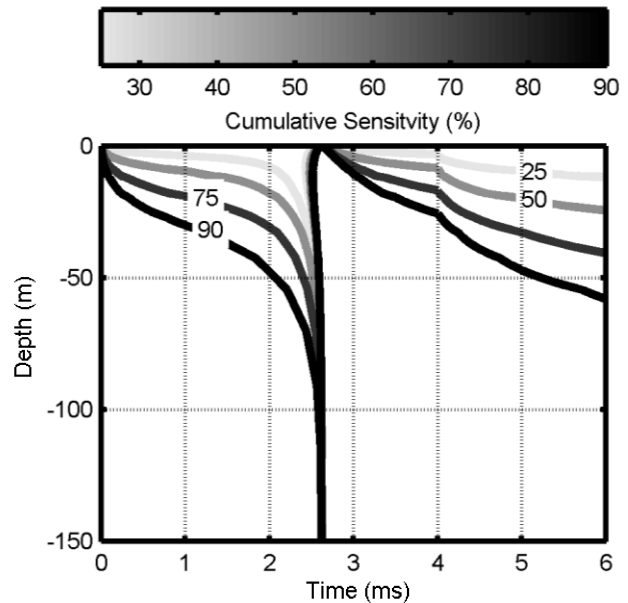

Figure 6: Cumulative sensitivity for a 1Ω m halfspace. The contour level indicates the portion of the receiver signal due to the (magnetic fields generated by) current located from surface to that depth.

more sensitive to the near-surface than off-time measurements.

EDITED REFERENCES
Note: This reference list is a copyedited version of the reference list submitted by the author. Reference lists for the 2015 SEG Technical Program Expanded Abstracts have been copyedited so that references provided with the online metadata for each paper will achieve a high degree of linking to cited sources that appear on the Web.

REFERENCES

Christensen, N. B., 1990, Optimized fast Hankel transform filters: Geophysical Prospecting, **38**, no. 5, 545–568. http://dx.doi.org/10.1111/j.1365-2478.1990.tb01861.x.

Hoversten, G. M., and H. F. Morrison, 1982, Transient fields of a current loop source above a layered earth: Geophysics, **47**, 1068–1077. http://dx.doi.org/10.1190/1.1441370.

Kaufman, A. A., and G. V. Keller, 1983, Frequency and transient soundings: Elsevier.

Lee, T., and R. Lewis, 1974, Transient EM response of a large loop: Geophysical Prospecting, **22**, no. 3, 430–444. http://dx.doi.org/10.1111/j.1365-2478.1974.tb00097.x.

Morrison, H. F., R. J. Phillips, and D. P. O'Brien, 1969, Quantitative interpretation of transient electromagnetic fields over a layered half space: Geophysical Prospecting, **17**, no. 1, 82–101. http://dx.doi.org/10.1111/j.1365-2478.1969.tb02073.x.

Nabighian, M., 1979, Quasistatic transient response of a conducting half-space — An approximate representation: Geophysics, **44**, 1700–1705. http://dx.doi.org/10.1190/1.1440931.

Pridmore, D. F., 1978, Three-dimensional modelling of electric and electromagnetic data using the finite element method: Ph.D. thesis, University of Utah.

Reid, J. E., and J. C. Macnae, 1998, Comments on the electromagnetic "smoke ring" concept: Geophysics, **63**, 1908–1913. http://dx.doi.org/10.1190/1.1444483.

Sengpiel, K. P., 1988, Approximate inversion of airborne EM data from a multilayered ground: Geophysical Prospecting, **36**, no. 4, 446–459. http://dx.doi.org/10.1111/j.1365-2478.1988.tb02173.x.

Singh, N. P., and T. Mogi, 2005, Electromagnetic response of a large circular loop source on a layered earth: A new computation method: Pure and Applied Geophysics, **162**, no. 1, 181–200. http://dx.doi.org/10.1007/s00024-004-2586-2.

Yin, C., and G. Hodges, 2007, 3D animated visualization of EM diffusion for a frequency-domain helicopter EM system: Geophysics, **72**, no. 1, F1–F7. http://dx.doi.org/10.1190/1.2374706.